

Pervaporation of the polydimethylsiloxane composite membranes filled with hydroxy-terminated silicone oil modified nano-silica

Wenwen Sun^{a,b}, Bingbing Li^{a,b,*}, De Sun^{a,b,*}, Hongwei Lin^c, Rui Xiao^{a,b}, Haotian Liu^{a,b}

^aSchool of Chemical Engineering, Changchun University of Technology, 2055 Yanan Street, Changchun 130012, P.R. China, Tel.: +8615526639820; email: lbingbing2002@163.com (B. Li), Tel.: +8615526639628; email: sundede@ccut.edu.cn (D. Sun), Tel.: +8613134455798; email: 2221915770@qq.com (W. Sun), Tel.: +8615568813910; email: 674425170@qq.com (R. Xiao), Tel.: +8616688212286; email: 425145158@qq.com (H. Liu)

^bKey Laboratory of Advanced Functional Polymer Membrane Materials of Jilin Province, 2055 Yanan Street, Changchun 130012, P.R. China

^cShanxi Coal and Chemical industry Group Shenmu Tianyuan Chemical industry Co., Ltd., Jinjie Industrial Park, Shenmu City, Shaanxi Province 719319, P.R. China, Tel.: +8615754368640; email: 2778870397@qq.com (H. Lin)

Received 10 April 2022; Accepted 2 December 2022

ABSTRACT

A new polydimethylsiloxane (PDMS) pervaporation membrane which filled hydroxy-terminated silicone oil modified nano-silica was prepared. Firstly, we used hydroxy-terminated silicone oil to modify nano-silica (OMNS); OMNS was used as a physical cross-linking agent to modify PDMS through blending OMNS into PDMS (OMNS-PDMS). OMNS particles were tested by Fourier-transform infrared spectroscopy and sedimentation experiments. It was found that the hydroxyl group in the silicone oil could condense with the carboxyl group on the surface of nano-silica (NS) to realize hydrophobic modification. Then, the OMNS-PDMS membrane morphology and tensile strength were investigated by scanning electron microscope and mechanical property tests. The OMNS-PDMS membrane showed significant advantages in flux and separation compared with the unfilled PDMS membrane. When the content of OMNS was 10 wt.%, the flow rate was 7 L/min, the permeate side was maintained at a vacuum pressure of 0.82 bar, and the feed ethanol concentration was 15 wt.%, the flux reached 682 g/(m²·h), and the pervaporation separation index reached 7099.74 g/(m²·h). Therefore, this work provides an excellent candidate method for pervaporation separation of dilute ethanol/water.

Keywords: Pervaporation; Hydroxy-terminated silicone oil; Nano-silica; Polydimethylsiloxane; Ethanol-water

1. Introduction

As one of the most promising energy-saving technologies, membrane separation technology has attracted more and more attention due to its environmental friendliness [1–8]. Pervaporation (PV) is a membrane separation technology used to separate organic/water systems and organic/organic systems [9,10]. Due to its broad application prospects in biochemical engineering, food industry,

environmental engineering, power electronics, and other fields [11,12]. As early as the 1950s, pervaporation of ethanol/water solution by membrane has been studied [13]. The introduction of PV technology in the alcohol fermentation process can improve the disadvantages of high energy consumption and low yield of the traditional approach. In the pervaporation process, the diffusion rate of water is often higher than that of ethanol [14,15]. Therefore, increasing the diffusion rate of alcohol in polymer membranes is one of the effective methods to improve PV

* Corresponding authors.

performance. Among the main PV membrane polymer materials, such as polydimethylsiloxane (PDMS), polyether block amides (PEBA), cross-linked poly(acrylate-co-acrylic acid), and polyvinylidene fluoride (PVDF) [16–23], PDMS has good flexibility due to its amorphous molecular structure and rubber state at ambient temperature. At the same time, it has higher flux for organics (such as acetone and ethyl acetate), stability, mechanical properties, chemical resistance, and thermal stability than other polymer membranes. It was also found that the unique free rotation of the Si–O bond improved the ethanol selectivity of PDMS membrane [24].

However, due to the low flux, traditional PDMS membranes are often unsatisfactory in practical industrial production. Liu et al. [25] prepared a polydimethylsiloxane-poly[(3,3,3-trifluoropropyl)methylsiloxane] (PDMS-PTF-PMS) block copolymer membrane to process ethanol/water mixtures, which can arrived 11.3 of ethanol separation factor and 1,149 g/m²·h of total flux for pervaporation recovery of 5 wt.% ethanol/water solution at 60°C. Cao et al. [26] prepared a polyhedral oligomeric silsesquioxane-graphene oxide/polydimethylsiloxane (POSS-GO/PDMS) membrane, the flux could reach 1346.9 g/m²·h with a separation factor of 11.2 when recovery of ethanol from 5 wt.% ethanol/water mixture.

Based on other scholars' studies, pervaporation requires at least a separation factor of 10.3 and a total flux of 150 g/m²·h to reach the market standard [27]. Therefore, it is essential to modify PDMS to improve the separation performance of ethanol/water. It has been reported that the properties of polymer membranes could be enhanced by introducing inorganic additives in the polymer solution [28,29]. Nano-silica filled polymer matrix composites have been received considerable attention in the past few years. It has been reported that nano-silica filled polymer matrix composites show a significant improvement in some respects, such as tensile strength, hardness, thermal properties, wear resistance, abrasion, and scratch resistance and opacity reducing [30]. Guo et al. [31] prepared a novel polyvinyl alcohol (PVA)-silica nanocomposite membrane using an *in-situ* sol-gel technique for pervaporative separation of water-ethylene glycol (EG) mixtures. Liu et al. [32] synthesized three-layer sandwich composite pervaporation membranes: the first layer next to the non-woven polyester fabric was PVA acetal. The middle layer was polyacrylamide (PAA)-Co-AN/SiO₂, and the surface layer was also PVA acetal. Zhao et al. proposed a novel method for fabricating polyelectrolyte complexes (PEC)-based nanohybrid membranes filled with SiO₂ [33]. The covalent and hydrogen bond between the silica particles and polymer chains increased their compatibility and cross-linking, which significantly enhanced the thermal stability and mechanical stability of the membranes [34]. But these composite membranes filled with SiO₂ mainly were used to water permeation.

In this study, we prepared functionalized silica nanoparticles via grafting method with hydroxy-terminated silicone oil (OH-TSO, modifier) and then PDMS composite membranes with different compositions of the hydroxy-terminated silicone oil modified nano-silica (OMNS) additive(OMNS-PDMS) for the ethanol pervaporation were prepared by solution casting method and the schematic

diagram of OMNS-PDMS membrane is shown in Fig. 1. The physical morphology, tensile strength, and thermal resistant performance of the OMNS-PDMS were systematically investigated. The effects of OMNS content and feed concentration were discussed for the pervaporation of dilute ethanol aqueous mixtures.

2. Experiment

2.1. Materials

PET non-woven fabrics as membrane support layers were obtained from Changzhou Haoxin Insulation Material Co., Ltd., (China). PDMS (Silicone Rubber 107, M_w5000), cross-linking agent ethyl silicate, and curing agent dibutyltin dilaurate were purchased from Shanghai Resin Company (China). Hydroxy-terminated silicone oil, nano-silica (95.68 m²/g, 50 nm), and reagent grade *n*-heptane were obtained from Shanghai Ruen Jie Chemical Reagent Company (China). Commercially supplied ethanol was used for pervaporation experiments without further purification.

2.2. Synthesis of OMNS

The synthesis mechanism of OMNS is shown in Fig. 2. Hydroxy-terminated silicone oil can be hydrolyzed into small molecules under acidic conditions. The hydrolyzed products react with the hydroxyl groups on the surface of SiO₂, changing SiO₂ from hydrophilic to hydrophobic [35]. The specific synthesis method is as follows: 3.64 g of nano-silica (NS) was first mixed in 150 mL of *n*-heptane under stirring for 30 min at room temperature. Then 12 wt.% concentrated sulfuric acid was added to adjust the pH to 4.7 and then 0.53 g hydroxy-terminated silicone oil was dropped in the mixture. The mixture was stirred by magnetic force for 30 min, heated in a 98°C oil bath for 60 min, and then aged naturally for 110 min. The mixture was filtered and dried at 60°C in a fume hood for 24 h to obtain the OMNS white powder.

2.3. Preparation of the unfilled PDMS membrane

The unfilled PDMS membranes were prepared by solution casting method. The casting solution was prepared by dissolving PDMS, cross-linker (ethyl silicate), and curing agent (dibutyltin dilaurate) in the solvent (*n*-heptane) with a ratio of 10:1:0.5 (in weight). The solution was then stirred for about 3 h to get homogeneous. After the preparation of the PDMS casting solution, it was poured onto the surface of PET non-woven fabric. Dried in a sterile room at room temperature for 24 h, the cross-linked unfilled PDMS flat sheet composite membrane was prepared. The total membrane thickness was about 130.0 ± 10 μm determined by a micrometer.

2.4. Preparation of the OMNS-PDMS membranes

The preparation process of the OMNS-PDMS membranes was carried out in the same way as in the case of the unfilled membrane (Section 2.3 – Preparation of the unfilled PDMS membrane). As shown in Fig. 3, after preparing the

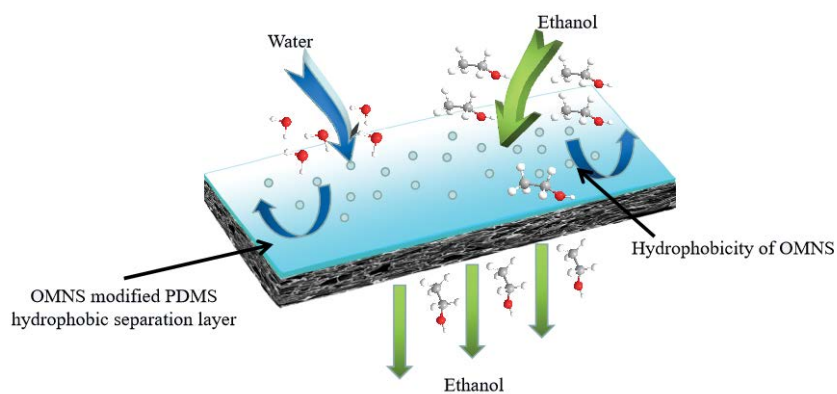


Fig. 1. Schematic diagram of OMNS-PDMS membrane.

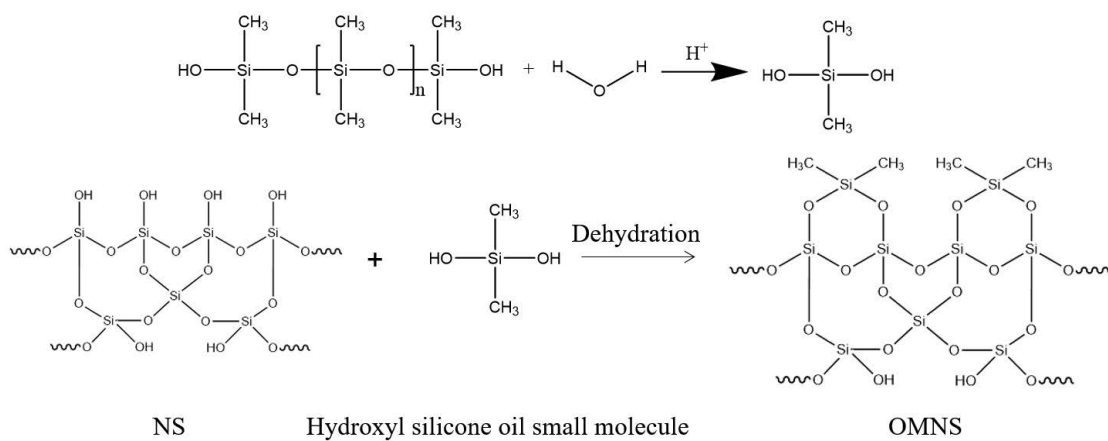


Fig. 2. Synthesis mechanism diagram of OMNS.

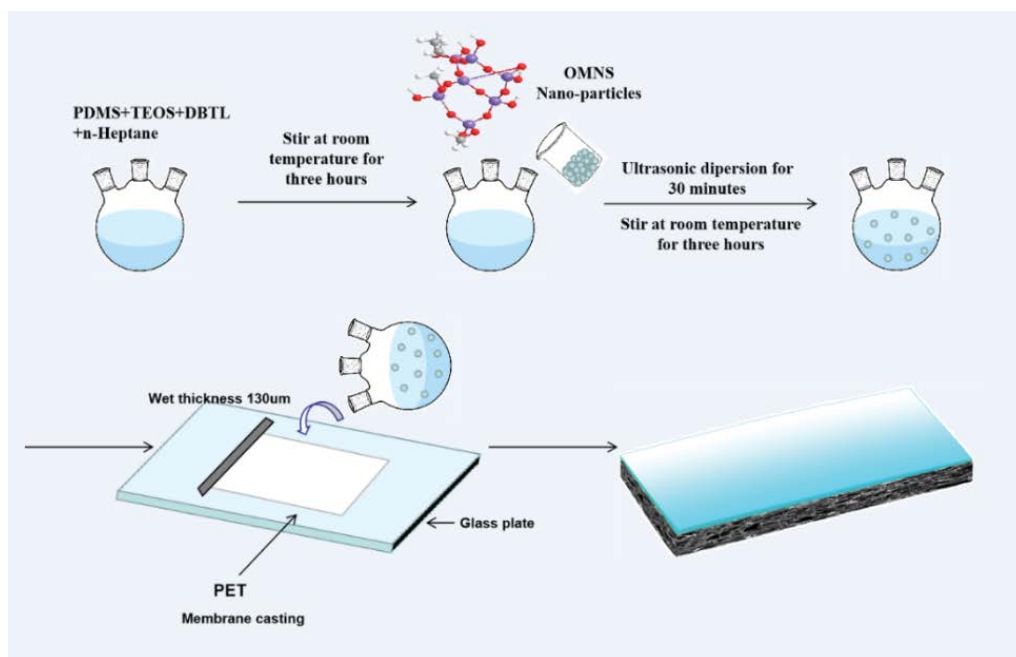


Fig. 3. Preparation process of the composite membrane.

unfilled PDMS casting solution, OMNS was evenly dispersed under stirring for 3 h before being treated with ultrasonic wave for 0.5 h. Then the OMNS filled PDMS casting solution was poured onto the PET non-woven fabric surface and stayed there for 15 s. Lastly, the OMNS filled PDMS coated flat sheet membrane was dried in the sterile room at room temperature for 24 h. The total membrane thickness was about $130.0 \pm 10 \mu\text{m}$ determined by a micrometer.

To investigate the effect of OMNS on the characterization and pervaporation performance of the PDMS membranes, the OMNS filled PDMS composite membranes with different content of OMNS were prepared. For simplicity, according to the OMNS content, membrane samples were designed as 5.0% OMNS-PDMS, 10.0% OMNS-PDMS, 20.0% OMNS-PDMS, 30.0% OMNS-PDMS. To study the influence of OMNS on the mechanical strength and thermal stability of the filled membranes, both unfilled and filled PDMS membranes without PET support were also prepared.

2.5. Characterization of OMNS and membranes

2.5.1. Surface hydroxyl number

0.4g OMNS, 5 mL absolute ethanol, and 15 mL 20 wt.% NaCl solution was dropped in a 100 mL beaker under stirring, then drop the pH value to 4.0 with 0.1 mol/L NaOH solution or 0.1 mol/L HCl. After that, 0.1 mol/L NaOH solution was added slowly to make the pH value rise to 9.0 and keep the pH value unchanged. According to Eq. (1), the number of hydroxyl groups (N) per square nanometer surface area of silica was calculated [37].

$$N = \frac{CVN_A \times 10^{-3}}{MS} \quad (1)$$

where C is the concentration of NaOH, 0.1 mol/L, V is the volume (mL) of NaOH consumed, N_A is the Avogadro constant, M is the mass of nano-silica (that is 0.4), and S is the specific surface area of OMNS measured by Brunauer–Emmett–Teller (BET), nm^2/g .

2.5.2. Settlement experiment

0.10 g ordinary nano-silica and 0.10 g modified nano-silica were put in two clean and dry test tubes, then 10 mL deionized water was injected and shaken. Then the tubes were put in an ultrasonic dispersing instrument for 30 min to disperse the nanoparticles and observe the settlement phenomenon.

2.5.3. Nitrogen adsorption

To detect the change of the specific surface area of OMNS, a nitrogen physical adsorption analysis experiment was carried out on OMNS samples. The pore size distribution of the OMNS was obtained by BJH (Barrett–Joyner–Halenda) model. In this experiment, TriStar II 3020 automatic specific surface and pore analyzer of American Micromeritics Company was used to measure the samples at 77 K. To eliminate the influence of impurities in the sample on the

experimental results, the sample is dried at 75°C for 10 h under the condition of the experimental instrument before the test.

2.5.4. Fourier-transform infrared spectroscopy

The samples' Fourier-transform infrared spectroscopy (FT-IR) spectra were recorded in the $500\text{--}4,000 \text{ cm}^{-1}$ range using a Nicolet-560 spectrometer (Nicolet, America).

2.5.5. X-ray diffraction

X-ray diffraction spectra of the OMNS were obtained at room temperature using a D-MAXIIA X-ray diffractometer (RIGAKU, Japan). The diffractograms were measured at a scanning speed of $10^\circ/\text{min}$ in the 2θ range of $5^\circ\text{--}60^\circ$ using a tube voltage of 40 kV and a tube current of 30 mA.

2.5.6. Scanning electron microscope characterization

The membrane samples were fractured in liquid nitrogen and then coated with gold to observe the surface and cross-section structures using scanning electron microscope (SEM; JEOL Model JSM-5600 LV, Japan).

2.5.7. Mechanical strength

To characterize the mechanical strength of OMNS filled PDMS membranes, the tensile strength measurements were performed on WSM25 KN Stress Testing System (Changchun Intelligent Instrument and Equipment Co., Ltd.).

2.5.8. Water contact angle measurement

The contact angle of water was measured by the JC2000D1 contact angle instrument (CA-D type, Shanghai Zhongcheng Digital Technology Instrument Co., Ltd., China). Water droplets (about $2 \mu\text{L}$ in volume) were placed on the membrane, and the water contact angle of the droplets was measured by system software.

2.6. Pervaporation performances

Fig. 4 shows the schematic diagram of the homemade pervaporation apparatus used in this case. PV experiments were conducted using a cross-flow laboratory scale membrane unit with a relatively small effective membrane area of $5.5 \times 10^{-3} \text{ m}^2$. Coupled with a large feed tank ($V = 3 \text{ L}$), it allowed the determination of the PV fluxes at almost constant feed concentration. 15 wt.% ethanol/water solution was used as feed keeping in the feed tank circulated by a circulation pump. The feed solution was pumped into the membrane cell with a high flow rate of 50 L/h to minimize the effect of concentration polarization. The feed tank was kept at a temperature of 60°C in a water bath. The permeate side was maintained at a vacuum pressure of 0.82 bar by vacuum pump. After the operation reached a steady state (about 1 h after starting), the permeate vapor samples were collected in a cold trap using liquid nitrogen. Then the sample was weighed and analyzed by gas chromatography with a thermal conductivity detector (TCD) (Techcomp LTD, GC7890). The calculation of the permeation flux (J),

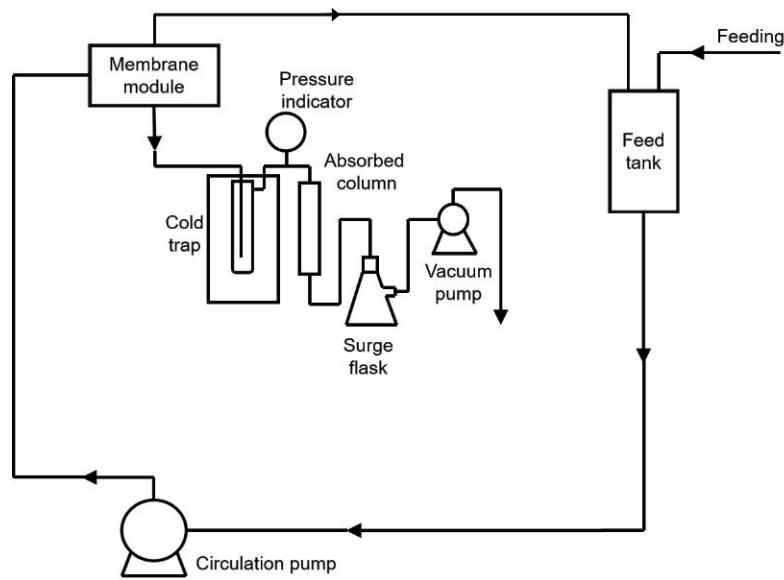


Fig. 4. Schematic diagram of pervaporation apparatus.

separation factor (α) and pervaporation separation index (PSI) is defined as:

$$J = \frac{m}{(\Delta t \cdot A)} \quad (2)$$

$$\alpha = \left(\frac{y_{\text{alcohol}} / y_{\text{water}}}{x_{\text{alcohol}} / x_{\text{water}}} \right) \quad (3)$$

$$\text{PSI} = (a - 1) \cdot J \quad (4)$$

where m is the total amount of permeate collected during the experimental time interval Δt of 1 h at steady state, A is the effective membrane area, x and y represent the mole fraction of a component in the permeate and the feed, respectively.

3. Result and discussion

3.1. Performance and characterization of OMNS nanoparticles

3.1.1. FT-IR spectra of OMNS

As shown in Fig. 5, 467 cm^{-1} is the characteristic absorption peak of Si–O bond, and 803 cm^{-1} was asymmetric stretching vibration peak of (Si–O–Si) bond; characteristic absorption peak of (Si–O–Si) bond at $1,100 \text{ cm}^{-1}$, the absorption peak of bound water at $1,630 \text{ cm}^{-1}$, the absorption peak at $3,420\text{--}3,450 \text{ cm}^{-1}$ was the stretching vibrations of (Si–OH) bond. The weak band at $2,970 \text{ cm}^{-1}$ was attributed to stretching vibration of Si–CH₃ and C–H group [36]. Compared with the infrared spectrum of NS, the intensity of peak at $3,430 \text{ cm}^{-1}$ was decrease on the spectrum of OMNS, however, the intensity of peak at $2,970 \text{ cm}^{-1}$ was increased, which was indicated that hydroxy silicone oil is grafted onto silica surfaces through reaction [38].

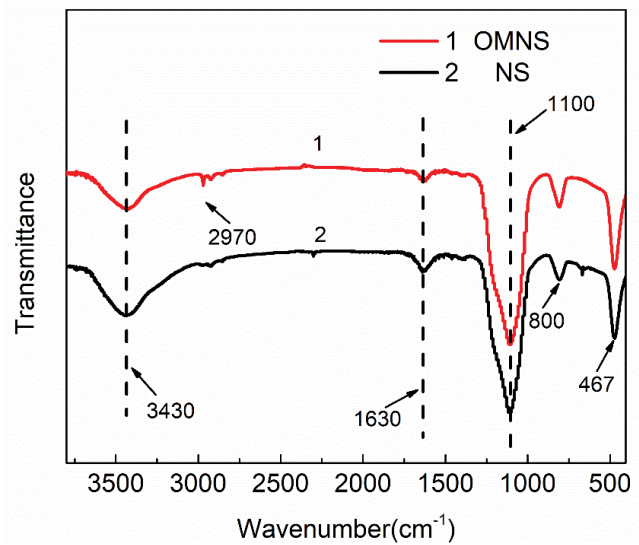


Fig. 5. FT-IR spectra of OMNS.

3.1.2. Nitrogen adsorption

Fig. 6a shows the isothermal nitrogen adsorption desorption curve of OMNS. In the relatively low pressure region of 0–0.1, there are a few micropores (less than 2 nm), there is an obvious hysteresis ring at 0.8, and the adsorption capacity increases sharply in the relatively high pressure region of 0.9–1.0, indicating that it has large mesoporous and macroporous structures (specific surface reached $95.68 \text{ m}^2/\text{g}$). According to Eq. (1), the number of hydroxyl groups (N) of NS are $8.07 \times 10^{18}/\text{g}$ and OMNS $5.22 \times 10^{18}/\text{g}$, which is proved that hydrophobic modification was successful for NS. Fig. 6b shows the pore volume and pore size distribution of OMNS. A small amount of distribution in

the near microporous area is less than 2 nm, while there is a large amount of distribution in the mesoporous and near mesoporous areas.

It shows the multi-level layered pore structure trend, reflecting the typical characteristics of mesoporous materials. Therefore, it can be predicted that the ability of OMNS to adsorb ethanol will be enhanced.

3.1.3. OMNS sedimentation experiment

In Fig. 7, A-1 represents the mixture of NS and deionized water, and A-2 represents the mixture of OMNS and deionized water. It can be seen in Fig. 7 that when the NS is added to water, it slowly sinks in the water. Due to many hydrophilic hydroxyl groups, nano-silica (NS) dispersed into water to form a white suspension. The nano-silica modified by silicone oil (OMNS) showed an unexpected effect. The interface layer between the OMNS and deionized water was obvious, and the OMNS was completely incompatible with water, which proved the success of hydrophobic modification. In addition, we also performed anhydrous ethanol precipitation experiments on NS (B-1) and OMNS (B-2). The results are shown in Fig. 7. Unmodified nano-silica is agglomerated, and it quickly sinks into the ethanol to cause insignificant delamination, while OMNS is compatible with the ethanol, and no agglomerated particles appear.

Set without layering, but mix with the ethanol evenly. It can be seen that OMNS has lipophilicity.

3.2. OMNS-PDMS membrane characterization

3.2.1. FT-IR analysis

Fig. 8 shows the FT-IR spectra of OMNS-PDMS membranes. As shown in Fig. 8, in the range of 500 to 4,000 cm^{-1} , the spectral peaks of all membranes are very similar, and the position of the characteristic peaks changes very little. The absorption peaks at 1,072 and 1,009 cm^{-1} represent the stretching vibration of the Si–O–Si group, the peak of 803 cm^{-1} represents the asymmetric stretching vibration of siloxane groups. And the peaks at 1,255 and 1,415 cm^{-1} represent the deformation vibration of two ($-\text{CH}_3$) groups on Si. The stretching vibration (Si–C) and (C–H) shows characteristic peaks in 2,850–2,970 cm^{-1} . Compared PDMS membrane with OMNS-PDMS membranes, there are no other new absorption peaks can be observed, which indicated that there was only a simple physical blending between OMNS and PDMS matrix during the filling process.

3.2.2. Water contact angle

Table 1 shows the surface water contact angle values for OMNS-PDMS membrane with different OMNS content.

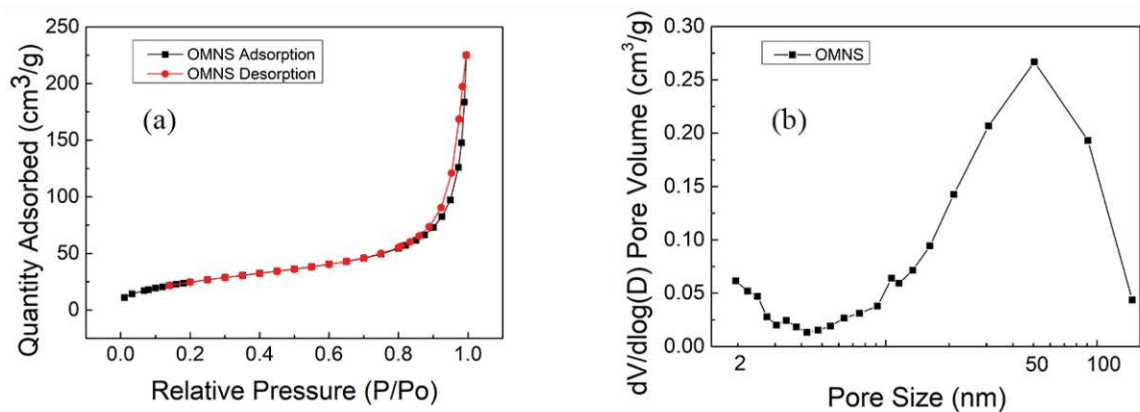


Fig. 6. BET analysis of OMNS.

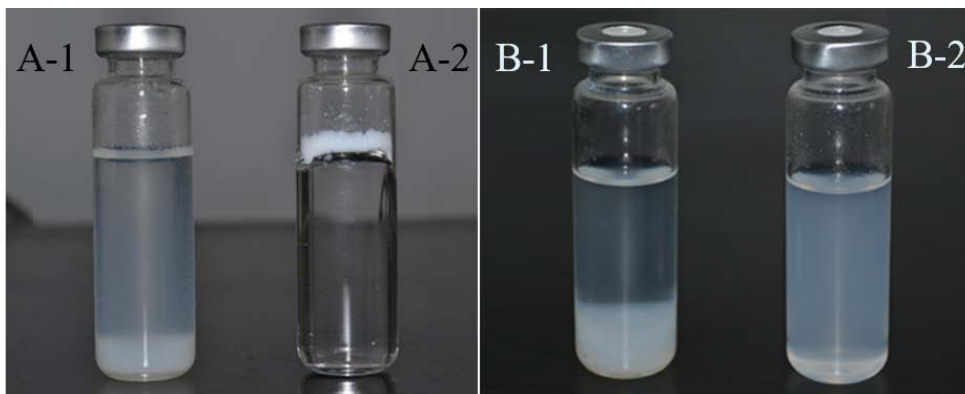


Fig. 7. Settlement experiments of OMNS.

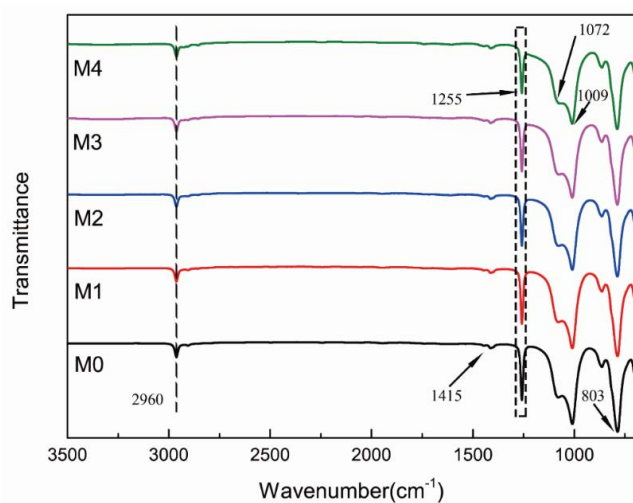


Fig. 8. FT-IR spectra of OMNS-PDMS membranes with various OMNS content.

Table 1
Water contact angle for OMNS filled PDMS membranes

Membranes	Contact angle
0.0% OMNS-PDMS	98.5°
5.0% OMNS-PDMS	103.7°
10.0% OMNS-PDMS	108.7°
20.0% OMNS-PDMS	110.9°
30.0% OMNS-PDMS	114.3°

When the OMNS content increases from 0% to 30%, the contact angle of the composite membranes surface increases from 98.5° to 114.3° because of the addition of hydrophobicity OMNS. The more OMNS filled, the stronger the hydrophobicity of the OMNS-PDMS membrane.

3.2.3. SEM analysis

To investigate the distribution of OMNS in the filled membranes, SEM characterization of the filled and unfilled membrane has been carried out. As a comparison, the PDMS membrane was filled with 20% unmodified nano-silica. As shown in Fig. 9, due to the good compatibility of the organic OMNS particles with the PDMS matrix, the OMNS was uniformly dispersed in the PDMS matrix. Therefore, no non-selective defect voids were found, and with the increase of OMNS, there were more and more OMNS particles on the surface of the OMNS-PDMS membrane. But for PDMS membrane filled with unmodified nano-silica, nano-silica agglomerated on the surface and in the cross-section.

3.2.4. X-ray diffraction analysis

Fig. 10 shows the X-ray diffraction (XRD) spectra of OMNS and OMNS-PDMS membranes. 17.6° and 22.9° diffraction peaks are amorphous peaks of non-woven fabrics [39]. The OMNS showed typical amorphous peaks at 22.59°–27.85° and the unfilled PDMS substrate membrane showed typical amorphous peaks at 11.91° and 25.47°. For filled PDMS membrane, with the increase of OMNS, the strength of the 25.47° amorphous peak is weakly enhanced which caused by the increase of crystallinity caused by the increase of OMNS in the PDMS membrane (Fig. 9).

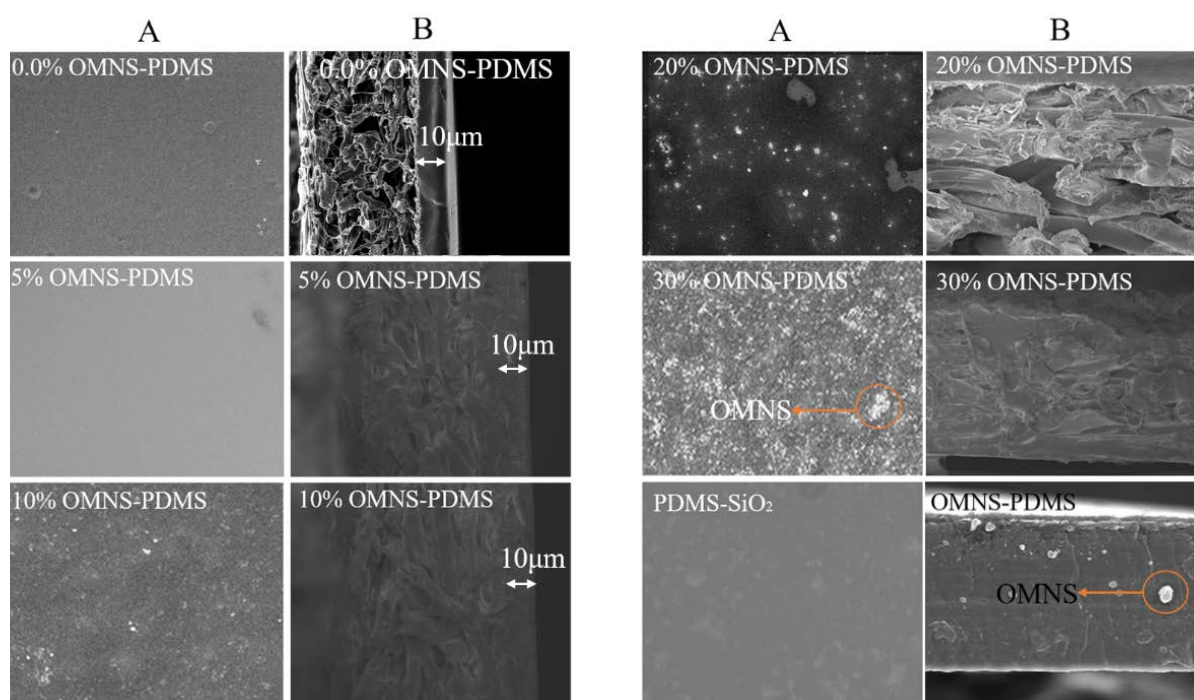


Fig. 9. SEM photographs of (A) top surface (5,000×) and (B) cross-section (400×) of the OMNS-PDMS composite membranes with different OMNS contents.

3.3. PV performance

The effect of different OMNS addition on the total flux, separation factor, and permeate separate index of PDMS composite membranes are shown in Fig. 11. All PDMS composite membranes filled with OMNS can offer significant advantages over unfilled PDMS membranes in flux and separation. Therefore, the proper filling of OMNS can increase the PV performance. As shown in Fig. 11a, with the increase of OMNS, the total flux of the composite membrane increased first and then decreased. This is mainly because OMNS is lipophilic, and more ethanol molecules can be preferentially adsorbed and diffused in the membrane. Therefore, the total flux of the membrane is increased. However, we also found that the flux decreased when the filling amount of OMNS was more significant than 10 wt.%. The reason is that the large OMNS with the specific surface area and mesoporous structure make water molecules and ethanol molecules penetrate through the membrane through a long and tortuous path, resulting in the decrease of the total flux. 10.0% OMNS-PDMS has the most significant total permeation flux, reaching 673.5 g/

(m²·h). The separation factor in Fig. 11b also shows the same trend. The separation factor of the composite membrane first increased then decreased.

When the OMNS content attained 20 wt.%, the separation factor reached 13.26. It was mainly due to the hydrophobicity of OMNS, and more ethanol molecules could be preferentially adsorbed and diffused in the membrane. By contrast, most water molecules were blocked out of the membrane. However, when the OMNS content attained 30 wt.%, the separation factor decreased quickly. This might be due to the poor compatibility between over-filled OMNS and PDMS membrane. Small defects in the composite membrane might lead to the low separation factor. Finally, we introduced PSI to evaluate the separation performance of the composite membrane, and the best performance was 20% OMNS-PDMS, the value reached 7,099.74 g/(m²·h).

4. Conclusion

A new composite membrane was developed for ethanol/water mixture pervaporation using PDMS membrane filled with hydroxyl silicone oil modified nano-silica (OMNS)

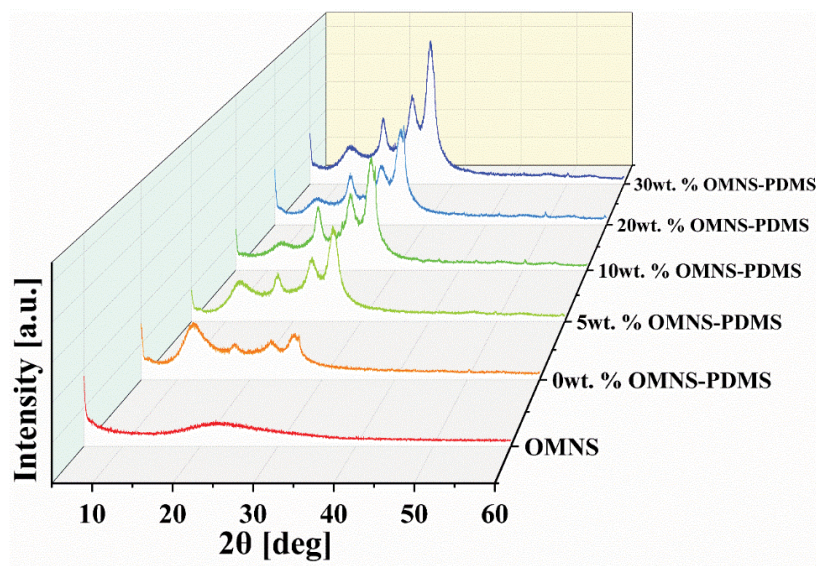


Fig. 10. XRD spectra of OMNS and OMNS-PDMS membranes.

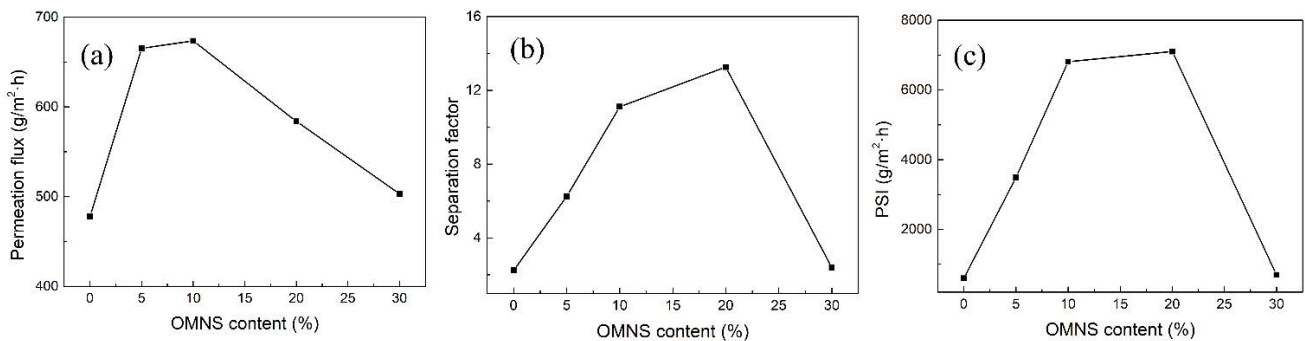


Fig. 11. The change of permeation flux (a), separation factor (b), and pervaporation separation index PSI (c) with different OMNS content.

as the top active layer and non-woven fabric as a support layer. Scanning electron microscopy showed that the OMNS-PDMS membranes were dense and had no apparent defects. OMNS was uniformly dispersed in the PDMS matrix. The FT-IR observation showed that OMNS was a simple physical blend in the matrix. The pervaporation performance of the PDMS membrane can be improved by adding OMNS. At a specific temperature and flow rate of ethanol concentration, 20.0% OMNS-PDMS membrane showed the best separation performance.

Acknowledgments

The authors gratefully acknowledge the National Key R&D Plan (grant numbers 2022YFB3903200, 2022YFB3903203), the Natural Science Foundation of Jilin Province (grant number 20210101392JC).

References

- N.L. Le, Y. Wang, T.-S. Chung, Pebax/POSS mixed matrix membranes for ethanol recovery from aqueous solutions via pervaporation, *J. Membr. Sci.*, 379 (2011) 174–183.
- S. Chovau, S. Gaykawad, A.J. Straathof, B. Van der Bruggen, Influence of fermentation by-products on the purification of ethanol from water using pervaporation, *Bioresour. Technol.*, 102 (2011) 1669–1674.
- N.R. Gopal, S.V. Satyanarayana, Cost analysis for removal of VOCs from water by pervaporation using NSGA-II, *Desalination*, 274 (2011) 212–219.
- J. Gu, X. Shi, Y. Bai, H. Zhang, L. Zhang, H. Huang, Silicalite-filled PEBA membranes for recovering ethanol from aqueous solution by pervaporation, *Chem. Eng. Technol.*, 32 (2009) 155–160.
- X. Jiang, J. Gu, Y. Shen, S. Wang, X. Tian, New fluorinated siloxane-imide block copolymer membranes for application in organophilic pervaporation, *Desalination*, 265 (2011) 74–80.
- X. Xu, D. Nikolaeva, Y. Hartanto, P. Luis, MOF-based membranes for pervaporation, *Sep. Purif. Technol.*, 278 (2021) 119233, doi: 10.1016/j.seppur.2021.119233.
- N. Moriyama, Y. Kawano, Q. Wang, R. Inoue, M. Guo, M. Yokoji, H. Nagasawa, M. Kanazashi, T. Tsuru, Pervaporation via silicon-based membranes: correlation and prediction of performance in pervaporation and gas permeation, *AIChE J.*, 67 (2021) e17223, doi: 10.1002/aic.17223.
- P. Peng, Y.Q. Lan, L. Liang, K. Jia, Membranes for bioethanol production by pervaporation, *Biotechnol. Biofuels*, 14 (2021) 10, doi: 10.1186/s13068-020-01857-y.
- F. Peng, F. Pan, D. Li, Z. Jiang, Pervaporation properties of PDMS membranes for removal of benzene from aqueous solution: experimental and modeling, *Chem. Eng. J.*, 114 (2005) 123–129.
- Y.K. Ong, G.M. Shi, N.L. Le, Y.P. Tang, J. Zuo, S.P. Nunes, T.-S. Chung, Recent membrane development for pervaporation processes, *Prog. Polym. Sci.*, 57 (2016) 1–31.
- S.V. Satyanarayana, A. Sharma, P.K. Bhattacharya, Composite membranes for hydrophobic pervaporation: study with the toluene–water system, *Chem. Eng. J.*, 102 (2004) 171–184.
- I. Prihatiningtyas, B. Van der Bruggen, Nanocomposite pervaporation membrane for desalination, *Chem. Eng. Res. Des.*, 164 (2020) 147–161.
- W.P. Silvestre, C. Baldasso, I.C. Tessaro, Potential of chitosan-based membranes for the separation of essential oil components by target-organophilic pervaporation, *Carbohydr. Polym.*, 247 (2020) 116676, doi: 10.1016/j.carbpol.2020.116676.
- N. Yu, T. Ando, C.M. Yun, Syntheses of siloxane-grafted aromatic polymers and the application to pervaporation membrane, *React. Funct. Polym.*, 67 (2007) 1252–1263.
- C.L. Chang, P.Y.J.D. Chang, Performance enhancement of silicone/PVDF composite membranes for pervaporation by reducing cross-linking density of the active silicone layer, *Desalination*, 192 (2006) 241–245.
- C. Ren, Z. Si, Y. Qu, S. Li, H. Wu, F. Meng, X. Zhang, Y. Wang, C. Liu, P. Qin, CF₃-MOF enhanced pervaporation selectivity of PDMS membranes for butanol separation, *Sep. Purif. Technol.*, 284 (2022) 120255, doi: 10.1016/j.seppur.2021.120255.
- G. Zhang, H. Cheng, P. Su, X. Zhang, J. Zheng, Y. Lu, Q. Liu, PIM-1/PDMS hybrid pervaporation membrane for high-efficiency separation of n-butanol–water mixture under low concentration, *Sep. Purif. Technol.*, 216 (2019) 83–91.
- H. Azimi, A. Ebneyamini, F.H. Tezel, J. Thibault, Separation of organic compounds from ABE model solutions via pervaporation using activated carbon/PDMS mixed matrix membranes, *Membranes*, 8 (2018) 40, doi: notepad.
- S. Liu, G. Liu, X. Zhao, W. Jin, Hydrophobic-ZIF-71 filled PEBA mixed matrix membranes for recovery of biobutanol via pervaporation, *J. Membr. Sci.*, 446 (2013) 181–188.
- H. Zhou, L. Lv, G. Liu, W. Jin, W. Xing, PDMS/PVDF composite pervaporation membrane for the separation of dimethyl carbonate from a methanol solution, *J. Membr. Sci.*, 471 (2014) 47–55.
- Z. Yang, S. Gao, Z. Cao, X. Chen, G. Yu, Recovery of ionic liquids from methanol by pervaporation with polydimethylsiloxane membrane, *Chem. Pap.*, 74 (2019) 1331–1337.
- C. Cheng, D. Yang, M. Bao, C. Xue, Spray-coated PDMS/PVDF composite membrane for enhanced butanol recovery by pervaporation, *J. Appl. Polym. Sci.*, 138 (2020) 49738, doi: 10.1002/app.49738.
- Y. Zhang, L. Lin, Q. Wang, R. Qiang, Y. Gao, S. Ma, Q. Cheng, Y. Zhang, Polyrotaxane cross-linked modified EC/PVDF composite membrane displaying simultaneously enhanced pervaporation performance and solvent resistance for benzene/cyclohexane separation, *J. Mater. Sci.*, 55 (2020) 8403–8419.
- P. Peng, B. Shi, Y. Lan, A review of membrane materials for ethanol recovery by pervaporation, *Sep. Sci. Technol.*, 46 (2010) 234–246.
- C. Liu, T. Xue, Y. Yang, J. Ouyang, P. Qin, Effect of cross-linker 3-methacryloxypropylmethylmethoxysilane on UV-cross-linked PDMS-PTFPMS block copolymer membranes for ethanol pervaporation, *Chem. Eng. Res. Des.*, 168 (2021) 13–24.
- T. Cao, J. Li, C. Li, N. Zhang, P. Cai, N. Wang, Q.-F. An, POSS-graphene oxide nanocomposite membranes for ethanol permeable pervaporation, *Microporous Mesoporous Mater.*, 331 (2022) 111635, doi: 10.1016/j.micromeso.2021.111635.
- D.J. O'Brien, L.H. Roth, A.J. McAloon, Ethanol production by continuous fermentation–pervaporation: a preliminary economic analysis, *J. Membr. Sci.*, 166 (2000) 105–111.
- Q. Zhao, J. Qian, C. Zhu, Q. An, T. Xu, Q. Zheng, Y. Song, A novel method for fabricating polyelectrolyte complex/inorganic nanohybrid membranes with high isopropanol dehydration performance, *J. Membr. Sci.*, 345 (2009) 233–241.
- S.-H. Chen, R.-M. Liou, C.-L. Lai, M.-Y. Hung, M.-H. Tsai, S.-L. Huang, Embedded nano-iron polysulfone membrane for dehydration of the ethanol/water mixtures by pervaporation, *Desalination*, 234 (2008) 221–231.
- M.M. Hasan, Y. Zhou, H. Mahfuz, S. Jeelani, Effect of SiO₂ nanoparticle on thermal and tensile behavior of nylon-6, *Mater. Sci. Eng., A*, 429 (2006) 181–188.
- R. Guo, X. Ma, C. Hu, Z. Jiang, Novel PVA–silica nanocomposite membrane for pervaporative dehydration of ethylene glycol aqueous solution, *Polymer*, 48 (2007) 2939–2945.
- X. Liu, Y. Sun, X. Deng, Studies on the pervaporation membrane of permeation water from methanol/water mixture, *J. Membr. Sci.*, 325 (2008) 192–198.
- Z. Qiang, The Machinability of Polyelectrolyte Complexes and The Construction of Functional Materials, Zhejiang University, Ph.D. Thesis, 2010 (in Chinese).
- H. Zhang, B. Li, D. Sun, X. Miao, Y. Gu, SiO₂-PDMS-PVDF hollow fiber membrane with high flux for vacuum membrane distillation, *Desalination*, 429 (2018) 33–43.

- [35] L. Jian, Z. Huang, X. Yan, W. Yuan, An OH-PDMS-modified nano-silica/carbon hybrid coating for anti-icing of insulators part I: fabrication and small-scale testing, *IEEE Trans. Dielectr. Electr. Insul.*, 23 (2016) 935–942.
- [36] I. Rahman, M. Jafarzadeh, C.J.C.I. Sipaut, Synthesis of organo-functionalized nano-silica via a co-condensation modification using γ -aminopropyltriethoxysilane (APTES), *Ceram. Int.*, 35 (2009) 1883–1888.
- [37] C.M.R. Wright, K. Ruengkajorn, A.F.R. Kilpatrick, J.-C. Buffet, D. O'Hare, Controlling the surface hydroxyl concentration by thermal treatment of layered double hydroxides, *Inorg. Chem.*, 56 (2017) 7842–7850.
- [38] L. Yang, S. Qiu, Y. Zhang, Y. Xu, Preparation of PDMS/SiO₂ nanocomposites via ultrasonical modification and miniemulsion polymerization, *J. Polym. Res.*, 20 (2012) 68, doi: 10.1007/s10965-012-0068-2.
- [39] Y. Li, Regulation of Crystallization and Toughening Behavior of Polyethylene Terephthalate, Ningxia University, Diss., 2019 (in Chinese).